NANO LETTERS

pubs.acs.org/NanoLett

Toward the Ultimate Limit of Phase Change in $Ge_2Sb_2Te_5$

R. E. Simpson,*,† M. Krbal,† P. Fons,*,†,‡ A. V. Kolobov,†,‡ J. Tominaga,† T. Uruga,‡ and H. Tanida‡

†Center for Applied Near-Field Optics Research, National Institute of Applied Industrial Science and Technology, Tsukuba Central4, 1-1-1 Higashi, Tsukuba 305-8562, Japan, and ‡SPring-8, Japan Synchrotron Radiation Research Institute (JASRI), Mikazuki Hyogo 679-5198, Japan

ABSTRACT The limit to which the phase change memory material $Ge_2Sb_2Te_5$ can be scaled toward the smallest possible memory cell is investigated using structural and optical methodologies. The encapsulation material surrounding the $Ge_2Sb_2Te_5$ has an increasingly dominant effect on the material's ability to change phase, and a profound increase in the crystallization temperature is observed when the $Ge_2Sb_2Te_5$ layer is less than 6 nm thick. We have found that the increased crystallization temperature originates from compressive stress exerted from the encapsulation material. By minimizing the stress, we have maintained the bulk crystallization temperature in $Ge_2Sb_2Te_5$ films just 2 nm thick.

KEYWORDS Phase change memory, $Ge_2Sb_2Te_5$, scaling, PCRAM, stress

The ever-increasing demand for greater memory densities is driving the development of new memory concepts and materials. Phase change RAM (PCRAM) is an emerging technology which, unlike silicon-based technologies, does not suffer from problems associated with the storage of charge.[1] $Ge_2Sb_2Te_5$ is the leading candidate material for such technology,[2] and in contrast to Si, "bits" of data are stored in the form of structural differences in a thin film of the material.

The ability of $Ge_2Sb_2Te_5$ to crystallize with speeds of less than 50 ns[3,4] and yet retain the amorphous state for durations of years may seem contradictory, but it is this important attribute which also allows the material to stably store data in cell volumes far less than those of electron trapping in silicon oxide. Changes in the rate of crystallization have been observed for films thinner than 30 nm; however, the true limit to which $Ge_2Sb_2Te_5$ can be scaled yet still retain the ability to change phase needs to be proven. Scaling $Ge_2Sb_2Te_5$ to smaller volumes has the added virtue that the switching power, accomplished by Joule heating, linearly improves with reducing cell size;[5] clearly this is beneficial with respect to the recent increase in portable devices which require large solid-state memories.

$Ge_2Sb_2Te_5$ can exist in two crystalline phases, the metastable cubic phase and the equilibrium hexagonal phase; in addition it can also exist in an amorphous phase. The cubic and hexagonal phases are formed by increasing the temperature of the as-deposited amorphous material to approximately 150 and 300 °C, respectively. The amorphous phase can be formed by either sputtering or rapid heating and quenching; the need for quench rates on the order of 10^{10} K s^{-1} have been reported.[6] Large optical and electrical differences manifest as a result of the atomic scale structural differences between the amorphous and cubic crystalline phases; generally, the crystalline phase exhibits a higher refractive index, optical absorption, and electrical conductivity in comparison to the amorphous phase. Thus changing phase between the amorphous and the metastable cubic crystalline state causes a large optical and electrical contrast which can be utilized in an optical disk or electrical memory.[7] The hexagonal crystalline phase is not utilized in $Ge_2Sb_2Te_5$ phase change memory, and therefore in this work we concentrate on the amorphous to cubic crystalline phase transition.

From a materials perspective the phase change properties are known to be fundamentally different as the thickness of the phase change material is reduced and the surface to volume ratio increased. Recently, efforts to grow single crystal $Ge_2Sb_2Te_5$ revealed that the $Ge_2Sb_2Te_5$ at the substrate interface is initially amorphous.[8] Further, the material which interfaces the $Ge_2Sb_2Te_5$ can change the crystal growth rate, activation energy,[9] threshold quench rate for amorphization, and the domain sizes.[10] Raoux et al. studied in situ X-ray diffraction from ultrathin films of $Ge_2Sb_2Te_5$, GeSb, and SbTe as a function of temperature.[11,12] It was found that for $Ge_2Sb_2Te_5$ films capped with Al_2O_3, the crystallization temperature sharply increased with decreasing film thickness while the crystal grain size decreased. From this analysis, the limiting film thickness for phase change was suggested to be 4 nm. However X-ray diffraction (XRD) measurement of very thin films at high temperature is challenging due to both the Debye−Waller effect and a reduction in the coherence length thus making definitive

* To whom correspondence should be addressed, robert.simpson@aist.go.jp and paul-fons@aist.go.jp.
Received for review: 08/25/2009
Published on Web: 12/30/2009

DOI: 10.1021/nl902777z | *Nano Lett.* **2010,** *10,* 414-419

conclusions difficult. In this paper we have employed two independent techniques, extended X-ray absorption fine structure (EXAFS) and ellipsometry, to investigate the crystallization as a function of film thickness. We have directly observed crystallization of films less than 4 nm thick and found that the crystallization temperature dependence on film thickness originates from stress within the $Ge_2Sb_2Te_5$ exerted from the encapsulation material.

EXAFS is an elementally selective technique which probes the local structure around a specific chemical species within a material. Typically only the first or second nearest neighboring atoms contribute to the EXAFS signal; hence the technique is sensitive to very thin films of material and monolayer measurements have been demonstrated.[13] The incident X-ray photons with energies larger than the core level electron binding energy of the target atom are absorbed allowing emission of photoelectrons which scatter from the neighboring atoms thus setting up a photoelectric standing wave which affects the X-ray absorption cross section of the excited atom leading to oscillations in absorption as a function of excitation energy. The different frequencies apparent in the oscillations are related to the separation of the neighboring atoms from the absorbing atom and can therefore be used to monitor changes in atomic positions. Background-subtracted EXAFS spectra as a function of momentum transfer are denoted as $\chi(k)$. The EXAFS spectra for the Ge K-edge in $Ge_2Sb_2Te_5$ shows significant, characteristic differences between the crystalline and amorphous states which have been attributed to an octahedral to tetrahedral coordination change in the Ge atom positions[14] and a corresponding change from resonant to covalent bonding.[15] These differences are most apparent at the momentum value $k = 3.3$ Å^{-1}; see Figure 1a. These spectra act as fingerprints for the different phases and can therefore be used to identify the state of the material. EXAFS spectra for films a few nanometers thick do not require the aforementioned, long coherence lengths of XRD and can be collected in minutes for a restricted k-range using third generation synchrotron sources. Thus in situ, temperature-dependent EXAFS is an ideal technique to determine the phase transition temperature of the Ge atom in $Ge_2Sb_2Te_5$ thin films.

To understand the effect of stress on thin films of $Ge_2Sb_2Te_5$, identical films were sandwiched with two different materials: $(ZnS)_{0.85}(SiO)_{0.15}$, commonly used in optical phase change media, and TiN, which is used to interface with $Ge_2Sb_2Te_5$ in electrical memory cells. The stress induced by both cladding materials was analyzed using a high-resolution X-ray diffractometer to measure the change in incident angle necessary to diffract from the (004) plane of a silicon substrate of thickness 650 μm. This technique is described elsewhere.[16] The induced stress was analyzed using Stoney's equation[17] via the induced substrate curvature; a Young's modulus, E, of 126 GPa and $\sigma = 0.3$ was used for the Poisson ratio[18] of the substrate. The films were 100 nm thick; as

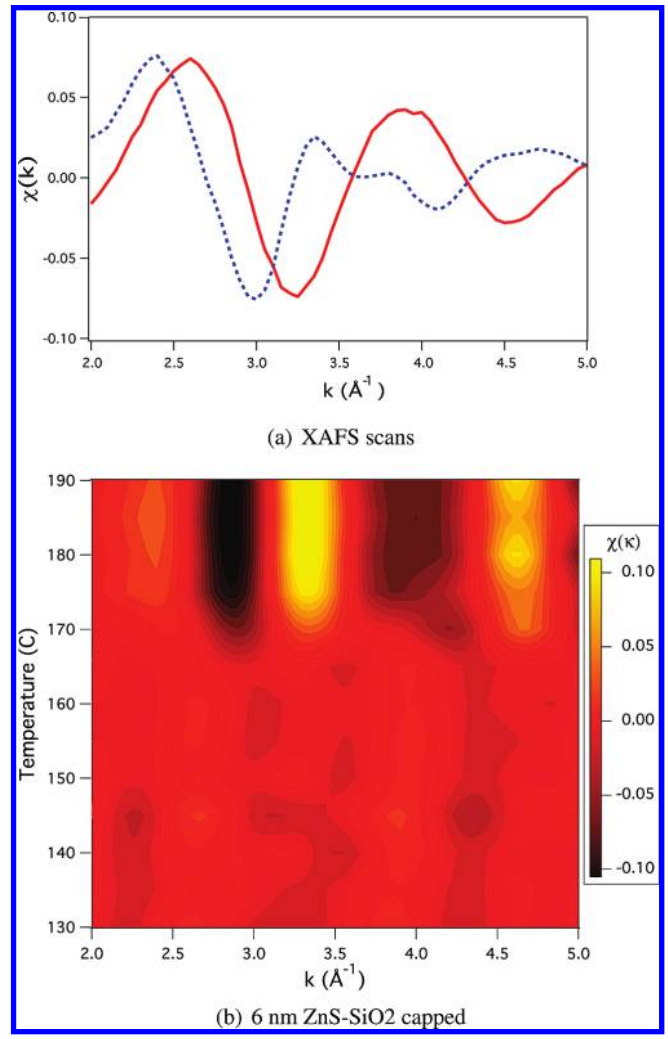

FIGURE 1. EXAFS spectra of amorphous (red curve) and 200 °C annealed (dashed blue curve) $Ge_2Sb_2Te_5$ samples (a) and the difference EXAFS spectra plotted as a function of temperature for 6 nm of $Ge_2Sb_2Te_5$ sandwiched between 20 nm of ZnS−SiO_2 film (b).

confirmed by X-ray reflectivity (XRR). Since the films were significantly less than 1 % of the substrate thickness, it was not necessary to employ any correction factors.[17] The calculated stress on the $Ge_2Sb_2Te_5$ layer from 20 nm thick films of $(ZnS)_{0.85}$ $(SiO)_{0.15}$ and TiN was found to be 58 and 240 MPa, respectively. $Ge_2Sb_2Te_5$ films of thicknesses varying between 2 and 10 nm were sputtered at 0.5 Pa and 30 W thus creating a $(ZnS)_{0.85}$ $(SiO)_{0.15}$ or TiN cladded structure atop of a quartz substrate; see Figure 2. The thickness, density, and surface roughness of the resultant structure was obtained by measuring XRR and fitting a model to the experimental data using the Motofit code.[19] The procedure allowed for subnanometer accurate measurements of all layers and the ability to check for the presence of interfacial phases. The XRR analysis confirmed that the density of the thin films and the interface roughness as a fraction of thickness remained constant implying that the films are continuous even at the thinnest extreme; the roughness of

DOI: 10.1021/nl902777z | *Nano Lett.* **2010,** *10,* 414-419

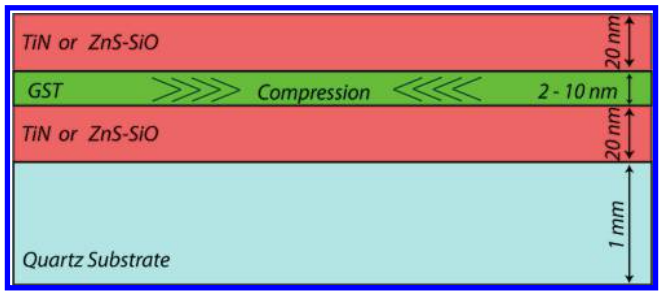

FIGURE 2. Diagram of samples used to measure the crystallization temperature of $Ge_2Sb_2Te_5$ as a function of film thickness. The $Ge_2Sb_2Te_5$ layer varies in thickness between 2 and 10 nm while the $(ZnS)_{0.85}$ $(SiO)_{0.15}$ or TiN encapsulation layers are kept constant at 20 nm thickness. The compressive stress, indicated, on the $Ge_2Sb_2Te_5$ is 58 and 240 MPa for $(ZnS)_{0.85}(SiO)_{0.15}$ and TiN, respectively.

the $Ge_2Sb_2Te_5$ layer typically corresponded to 30% of the total film thickness.

EXAFS spectra between 130 and 200 °C were collected at intervals of 5 °C. During the measurement the sample temperature was held constant and controlled to within 1 °C. Soller slits and Al filters were put between the sample and a muliple element solid-state detector to suppress any background fluorescence and the resultant scans were Fourier filtered using the Athena[20] program before subtracting the 130 °C scan to emphasize subsequent changes in the spectra. A change in atomic structure is evident as a large change in χ at a particular temperature; for thicker films this change took place at approximately 170 °C, see Figure 1b. To complement these measurements, temperature-dependent ellipsometry at 633 nm was also carried out on the films for the fixed angle of 70 °C. Combining both ellipsometry and EXAFS measurements as a function of temperature allows investigation of both atomic structural changes as well as the resultant optical changes. At the phase transition, the ellipsometric parameters, Δ and Ψ, which are related to the change in phase between the P and S polarization states upon reflection, show a discontinuity which arises due to a convoluted effect of changes in the material's dielectric properties and thickness. For the case of ultrathin films on the order of a few nanometers thick, the ellipsometric signal is dominated by interfacial effects; the interfacial sensitivity of ellipsometry has been utilized in the literature to investigate monolayer films that would otherwise be difficult to characterize.[21] In general, the temperature at which crystallization occurs is dependent on the film thickness and the material which confines it. A clear trend is observed whereby the crystallization temperature of $Ge_2Sb_2Te_5$, enclosed by TiN, rapidly increases from 165 to 299 °C for films of thickness decreasing from 6 to 2 nm. A similar trend was observed by Raoux et al. for $Ge_2Sb_2Te_5$ capped by Al_2O_3.[11] The results of both temperature-dependent EXAFS and ellipsometry have been plotted on the same axes in Figure 3a. Interestingly, this increase in crystallization temperature is not a universal observation for all cladding materials; enclosing the $Ge_2Sb_2Te_5$ layer with $(ZnS)_{0.85}(SiO)_{0.15}$ seems

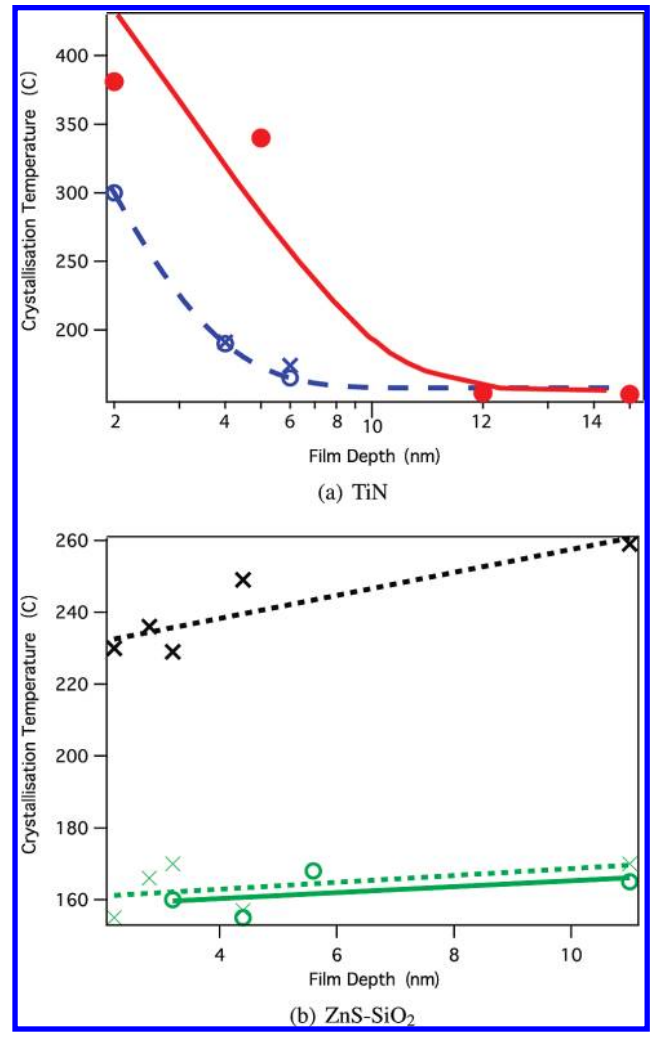

FIGURE 3. Crystallization temperature as a function of film thickness. The results for the cladding materials TiN and published data for Al_2O_3[11] are shown in (a). The effect of the lower stress cladding material ZnS−SiO_2 is given in (b). (red solid circle) Al_2O_3 using XRD, (red solid line) Al_2O_3 fit, (blue open circle) TiN using EXAFS, (blue ×) TiN using ellipsometry, (blue dashed line) TiN fit, (black ×) $(ZnS)_{0.85}(SiO)_{0.15}$ clad hex phase using ellipsometry, (black dashed line) $(ZnS)_{0.85}(SiO)_{0.15}$ cladding hex using ellipsometry fit, (green ×) $(ZnS)_{0.85}(SiO)_{0.15}$ cladding cubic phase using ellipsometry, (green dashed line) $(ZnS)_{0.85}(SiO)_{0.15}$ cladding cubic phase ellipsometry fit, (green ×) cubic phase using EXAFS, (green solid line) cubic phase using EXAFS fit. (Error bars are less than the marker size.)

to allow the material to crystallize at temperatures close to those reported for thicker films and, in contrast, a small decrease in the crystallization temperature could be achieved by reducing the $Ge_2Sb_2Te_5$ thickness from 6 to 2 nm. A second discontinuity is also observed in the ellipsometric parameters at temperatures decreasing from 259 to 229 °C as the film thickness was reduced to 2 nm; corresponding to temperature range of the cubic-hexagonal phase transition. These results have been plotted in Figure 3.

The crystallization temperature changes as a function of the $Ge_2Sb_2Te_5$ layer's thickness; see Figure 3. A major difference between ultrathin films and thicker films is the increased proportion of atoms at the interface. The interfa-

DOI: 10.1021/nl902777z | *Nano Lett.* **2010,** *10,* 414-419

cial atoms experience a biaxial stress, acting tangentially along the films surface, from forces originating within the cladding layers.[22] Thus for the thinnest films, a greater proportion of the $Ge_2Sb_2Te_5$ atoms are at the interface and the stresses within the cladding material have a greater influence on the properties of the $Ge_2Sb_2Te_5$ film. Interfacial mixing has been reported for GeSb films[12] whereby the cladding material effectively dopes the phase change film causing a change in its properties. Despite the 30% interfacial roughness measured for the films, the EXAFS results show the same structural transition occurs during crystallization irrespective of the $Ge_2Sb_2Te_5$ film thickness and, therefore, degree of interfacial mixing. Further, EXAFS measurements monitor the local structure about the Ge atom and the structure shows no apparent changes due to interfacial mixing; therefore we believe that, in the case of $Ge_2Sb_2Te_5$, its effect on the transition temperature is minimal. In this study, TiN was found to increase the crystallization temperature whereas, $(ZnS)_{0.85}(SiO)_{0.15}$ allows the $Ge_2Sb_2Te_5$ to crystallize at slightly lower temperatures with decreasing film thickness. The glass transition temperature, T_g, is the minimum temperature at which atoms within an amorphous matrix can rearrange to form lower free energy, amorphous structures[23] and can therefore be considered the temperature at which a solid material is transformed into a high viscosity liquid.[24] At the glass transition temperature the stresses within the $Ge_2Sb_2Te_5$ film are reduced by viscous flow, and this has been observed above 100 °C for uncapped $Ge_2Sb_2Te_5$.[25] If a tensile stress is applied to $Ge_2Sb_2Te_5$, the pressure within the $Ge_2Sb_2Te_5$ film will be reduced and conversely increased in the case of compression. As mentioned earlier, the stress induced from the cladding layers of the $Ge_2Sb_2Te_5$ films in this experiment was found, in the case of 20 nm of TiN, to be 240 MPa. This magnitude of stress is expected to play a contributing role in the crystallization process. It is known that the cubic crystalline phase of $Ge_2Sb_2Te_5$ contains approximately 10% vacancies.[26] Upon crystallization, $Ge_2Sb_2Te_5$ undergoes a 5% volume reduction which might suggest that a compressive stress or pressure would aid the crystallization process; however, an observed increase in crystallization temperature suggests otherwise. Two factors are considered which could cause the increased crystallization temperature: (1) an increase in activation energy; (2) a requirement of vacancies in the crystallized phase.

The transition of the Ge atom from a tetrahedral to octahedral coordination during crystallization is known to be an activated process with an associated energy E_g of 2.3 eV.[27] Published data have shown that the crystallization activation energy can increase with decreasing film thickness.[28] In such a case, the compression originating from the cladding restricts the crystallization kinetics by increasing the activation barrier between the two phases, perhaps by diminishing the process of covalent bond rupturing during the passage of the Ge atom from tetrahedral to octahedral Te coordination. Higher temperatures are therefore necessary for the material to crystallize; this explains the increase in crystallization temperature for $Ge_2Sb_2Te_5$ compressed by TiN. Similar activation energy increases have also been observed when $Ge_2Sb_2Te_5$ is doped with nitrogen.[29] In such cases, a change in the size of the cubic lattice is observed indicating the presence of intrinsic stress.[30] Until now these effects have not been correlated, but we believe stress could be a possible explanation for the observed increase in activation energy. For films less than 1 nm in thickness, the proportion of vacancies at the $Ge_2Sb_2Te_5$−substrate interface is lower than the proportion of vacancies within the bulk of the film and this restricts interface crystallization.[8] Now addressing point (2), we believe there is a threshold density of $Ge_2Sb_2Te_5$ above which crystallization cannot occur due to the necessity for the creation of vacancies in the cubic phase. It follows that there is a minimum unit cell volume necessary for crystallization of $Ge_2Sb_2Te_5$. We have previously shown that the $Ge_2Sb_2Te_5$ cubic unit cell cannot support vacancies when hydrostatic pressure is greater than 15 GPa, corresponding to a threshold unit cell volume, V_{th} of 180 Å^3.[31] Therefore the volume of 180 Å^3 is extremely important; it is the minimum quantity of $Ge_2Sb_2Te_5$ which can support sufficient vacancies to allow transformation into the cubic phase, and since electronic properties are dominated by short-range atomic order,[32] structural changes on this scale would also result in electrical contrast between structural phases. However resonant bonding is also required to form the cubic crystalline structure.[15] There must be a minimum thickness over which the atomic environment is sufficiently symmetric to satisfy the requirement for resonant bonding. Should the cell become less than this critical size, the reduction in symmetry will make the cubic crystal unstable. In the samples used in our EXAFS and ellipsometry experiments the interface roughness was found to be 30%. It is therefore reasonable to assume that for the 2 nm thick films, a symmetric bonding environment is maintained over 1.4 nm in depth. This seems to suggest that at least two unit cells (each with width 0.6 nm[31]) can satisfy resonant bonding in one dimension. From this we can speculate that a volume containing at least eight unit cells is necessary to stabilize the cubic structure through resonant bonding and therefore the minimum volume of $Ge_2Sb_2Te_5$ which can be implemented in phase change RAM is around 1.7 nm^3; intermediate range order is necessary. The surface energy of such a small cluster of atoms would play an increasingly dominant role in the phase change process by effectively reducing the vacancy formation energy;[33] therefore careful selection of the interfacial material would be necessary to stabalize the amorphous phase. Phase change of such a small volume is only possible as a consequence of the Ge tetrahedral−octahedral flip which occurs on a local atomic scale;[14] long-range ordering is a corollary of this transition and not a necessity for crystallization. In this paper a maximum compression of 240 MPa was reported; refer-

DOI: 10.1021/nl902777z | Nano Lett. 2010, 10, 414-419

ring again to ref 31, the unit cell volume is greater than V_{th} for this pressure. Therefore the increased energy required for crystallization is explained by the increased activation energy for the Ge atom to transit into the octahedrally coordinated position rather than a suppression of vacancies.

To aid the understanding of how stresses acting on nanoscale $Ge_2Sb_2Te_5$ cells can affect the phase change performance of the material, it is informative to consider the thermodynamic cycle of the phase change process. From room temperature, T_1, the film is heated and therefore expands thus doing work against the cladding materials. The work done in changing phase is dependent on the stress acting on the $Ge_2Sb_2Te_5$ from cladding materials. Clearly, a material such as $(ZnS)_{0.85}(SiO)_{0.15}$, allows the $Ge_2Sb_2Te_5$ to expand with less resistance than TiN and the increase in pressure within the $Ge_2Sb_2Te_5$ is small. Conversely, TiN, strongly resists the thermal expansion of $Ge_2Sb_2Te_5$ thus reducing the thermal expansion coefficient of the film. Once the $Ge_2Sb_2Te_5$ reaches its crystallization temperature, T_x, a rapid contraction occurs, relieving pressure and stresses acting from the cladding materials. The crystallization is a stress-dependent, activated process and therefore T_x is dependent on the magnitude of stress from the encapsulation materials. Now, in the crystalline phase, $Ge_2Sb_2Te_5$ once again expands with increasing temperature and pressure builds up as the cladding materials oppose the expansion. Again the amount of energy spent on thermal expansion of the crystallized film is dependent on the magnitude of stress within the $Ge_2Sb_2Te_5$. At the melting point, the material's rate of thermal expansion increases. Once at the maximum temperature of the melt, the heat source is removed and the material rapidly quenches into the amorphous phase and, in so doing, solidifies at the glass transition temperature, T_g, causing a change in the rate of contraction. From T_g the material can gently cool back to room temperature, T_1, completing the cycle. This cycle is depicted in Figure 4 for a film under compression.

The work done by the $Ge_2Sb_2Te_5$ on the cladding material is the path integral around the phase change cycle. The initial work done in going from T_1 to the crystallization temperature is greater when the $Ge_2Sb_2Te_5$ experiences higher compressive stress, and in such a scenario the activation energy for crystallization is greater. However, after crystallization, the $Ge_2Sb_2Te_5$ does not expand to the same extent as a material which is under tensile or lower compressive stress; hence the total work done on the cladding material through the whole cycle is less. The reduction in total work done by the $Ge_2Sb_2Te_5$ on the cladding material for encapsulation which induces high compressive stress in the $Ge_2Sb_2Te_5$ is expected to prolong the write/erase cyclability. Further, the higher crystallization temperature and crystallization activation energy mean that scaling to smaller dimensions will actually increase the stability of the amorphous state hence improving the longevity of the strored data. These improvements do, however, come at some cost,

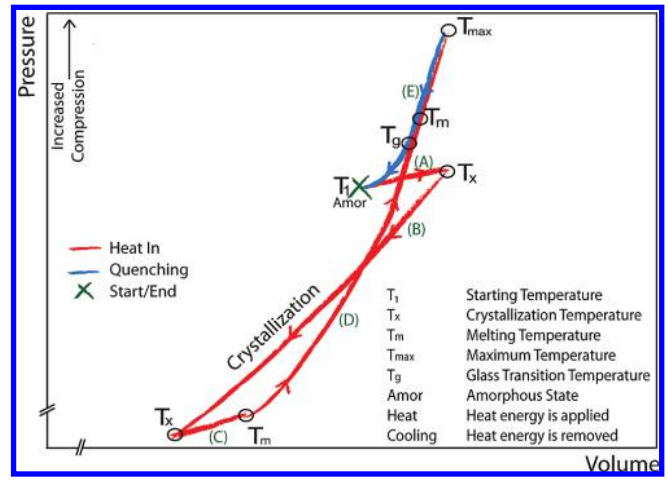

FIGURE 4. The thermodynamic cycle for phase change materials under compressive stress: (A) thermal expansion of amorphous phase; (B) crystallization; (C) thermal expansion of the crystalline phase; (D) thermal expansion of the molten phase; (E) quenching of the molten phase back into amorphous.

higher crystallization temperatures and hence greater power requirements.

Proper analysis of the phase change thermodynamic cycle and consideration of the stress applied by the cladding layers allow one to formulate principles of design for increasingly small memory scales. If, for example, sub-10-nm $Ge_2Sb_2Te_5$ memory cells are to be implemented to replace nonvolatile, charge storage, Flash-type memories, the issue of cyclability is arguably of less importance than that of electrical efficiency and therefore a cladding material which minimizes the crystallization temperature by reducing the compressive stresses on the $Ge_2Sb_2Te_5$ would be more appropriate. However, if electrical efficiency is of lower importance and cyclability is the prime goal of the memory cell, a highly compressive cladding material, like TiN, would be more suitable. This would be the case for DRAM replacement where essentially an infinite number of cycles are required. A highly compressive cladding material has the added advantage that the energy required to crystallize the material increases with decreasing cell dimensions and therefore aids the problems associated with thermal cross-talk and archival stability of the materials; this is opposite to conventional DRAM.

In conclusion, the cladding layers surrounding the $Ge_2Sb_2Te_5$ play an increasingly important role as the cell dimensions are reduced below 10 nm. It is critical that the volume of $Ge_2Sb_2Te_5$ is sufficient to maintain vacancies and stabilization through resonant bonding in the cubic phase. Films just 2 nm thick are able to crystallize; we believe this is close to the minimum thickness which resonant bonding is capable of stabilizing the cubic phase. We have found that compressive stress increases the energy required for the transition of the Ge atoms from tetrahedral to octahedral coordination thus increasing the crystallization temperature. Materials such as TiN and Al_2O_3 tend to cause a sharp

DOI: 10.1021/nl902777z | *Nano Lett.* **2010,** *10,* 414-419

increase in the crystallization temperature whereas $(ZnS)_{0.85}(SiO)_{0.15}$ which applies a lower stress has a negligible effect on the crystallization temperature. These insights have allowed us to identify essential design criteria to enable $Ge_2Sb_2Te_5$ memory cells to be scaled to their physical, phase change limit.

Acknowledgment. A part of the work was supported by METI Innovation Research Projects on Nanoelectronics Materials and Structures. The EXAFS measurements were performed at Spring 8 BL01B1 under proposal: 2008B1202. R. E. Simpson and M. Krbal would like to acknowledge the support of the Japanese Society for the Promotion of Science for their current research fellowships.

REFERENCES AND NOTES

(1) Bez, R.; Pirovano, A. *Mater. Sci. Semicond. Process.* **2004**, *7*, 349–355, Papers presented at the E-MRS 2004 Spring Meeting Symposium C: New Materials in Future Silicon Technology.
(2) Wuttig, M.; Yamada, N. *Nat. Mater.* **2007**, *6*, 824–832.
(3) Bez, R.; Gleixner, R. J.; Pellizzer, F.; Pirovano, A.; Atwood, G. In *Phase Change Materials: Science and Applications*; Raoux, S., Wuttig, M., Eds.; Springer Verlag: Berlin, 2008; Chapter *16*, pp 355−380.
(4) Yamada, N.; Ohno, E.; Nishiuchi, K.; Akahira, N.; Takao, M. *J. Appl. Phys.* **1991**, *69*, 2849–2856.
(5) Pirovano, A.; Lacaita, A. L.; Benvenuti, A.; Pellizzer, F.; Hudgens, S.; Bez, R. Scaling analysis of phase-change memory technology. *Tech. Dig.—Int. Electron Devices Meet.*, **2003**
(6) Peng, C.; Cheng, L.; Mansuripur, M. *J. Appl. Phys.* **1997**, *82*, 4183–4191.
(7) Welnic, W.; Botti, S.; Reining, L.; Wuttig, M. *Phys. Rev. Lett.* **2007**, *98*, 236403.
(8) Braun, W.; Shayduk, R.; Flissikowski, T.; Ramsteiner, M.; Grahn, H. T.; Riechert, H.; Fons, P.; Kolobov, A. *Appl. Phys. Lett.* **2009**, *94*, No. 041902.
(9) Ohshima, N. *J. Appl. Phys.* **1996**, *79*, 8357–8363.
(10) Ohshima, N. *J. Appl. Phys.* **1998**, *83*, 5244.
(11) Raoux, S.; Jordan-Sweet, J. L.; Kellock, A. J. *J. Appl. Phys.* **2008**, *103*, 114310.
(12) Raoux, S.; Cheng, H.-Y.; Jordan-Sweet, J. L.; Munoz, B.; Hitzbleck, M. *Appl. Phys. Lett.* **2009**, *94*, 183114.
(13) Schedel-Niedrig, T.; Weiss, W.; Schlogl, R. *Phys. Rev. B* **1995**, *52*, 17449–17460.
(14) Kolobov, A.; Fons, P. A.; Frenkel, J. T.; Ankudinov, A. L.; Uruga, T. *Nat. Mater.* **2004**, *3*, 703–708.
(15) Shportko, K.; Kremers, S.; Woda, M.; Lencer, D.; Robertson, J.; Wuttig, M. *Nat. Mater.* **2008**, *7*, 853–858.
(16) Yu, Y.; Lai, M.; Lu, L.; Yang, P. *J. Alloys Compd.* **2008**, *449*, 56–59, The First International Symposium on Functional Materials (ISFM2005).
(17) Janssen, G.; Abdalla, M.; van Keulen, F.; Pujada, B.; van Venrooy, B. *Thin Solid Films* **2009**, *517*, 1858–1867.
(18) Franca, D. R.; Blouin, A. *Meas. Sci. Technol.* **2004**, *15*, 859–868.
(19) Nelson, A. *J. Appl. Crystallogr.* **2006**, *39*, 273–276.
(20) Ravel, B.; Newville, M. *J. Synchrotron Radiat.* **2005**, *12*, 537–541.
(21) Prime, K.; Whitesides, G. *Science* **1991**, *252*, 1164–1167.
(22) Harsha, K. S. *Nucleation and Growth of Films*, 1st ed.; Elsevier: Amsterdam, 2005.
(23) Lankhorst, M. *J. Non-Cryst. Solids* **2002**, *297*, 210–219.
(24) Rao, K. *Structural Chemistry of Glasses Structural Chemistry of Glasses*; Elservier: Amsterdam, 2002.
(25) Park, I.-M.; Jung, J.-K.; Ryu, S.-O.; Choi, K.-J.; Yu, B.-G.; Park, Y.-B.; Han, S. M.; Joo, Y.-C. *Thin Solid Films* **2008**, *517*, 848–852.
(26) Wuttig, M.; Lüsebrink, D.; Wamwangi, D.; Welnic, W.; Gillessen, M.; Dronskowski, R. *Nat. Mater.* **2007**, *6*, 122–128.
(27) Tominaga, J.; Shima, T.; Fons, P.; Simpson, R.; Kuwahara, M.; Kolobov, A. *Jpn. J. Appl. Phys* **2009**, *48*, No. 03A053.
(28) Wei, X.; Luping, S.; Chong, C. T.; Rong, Z.; Koon, L. H. *Jpn. J. Appl. Phys.* **2007**, *46*, 2211–2214.
(29) Privitera, S.; Rimini, E.; Zonca, R. *Appl. Phys. Lett.* **2004**, *85*, 3044–3046.
(30) Do, K.; Sohn, H.; Ko, D.-H. *J. Electrochem. Soc.* **2007**, *154*, H867–H870.
(31) Kolobov, A. V.; Haines, J.; Pradel, A.; Ribes, M.; Fons, P.; Tominaga, J.; Katayama, Y.; Hammouda, T.; Uruga, T. *Phys. Rev. Lett.* **2006**, *97*, No. 035701.
(32) Weaire, D.; Thorpe, M. F. *Phys. Rev. B* **1971**, *4*, 2508–2520.
(33) Qi, W. H.; Wang, M. P. *Physica B* **2003**, *334*, 432–435.

DOI: 10.1021/nl902777z | *Nano Lett.* **2010,** *10,* 414-419